33rd Annual International Conference of the IEEE EMBS
Boston, Massachusetts USA, August 30 - September 3, 2011

Reconstruction of Multiple Gastric Electrical Wave Fronts Using Potential Based Inverse Methods

J. H. K. Kim, A. J. Pullan, and L. K. Cheng

Abstract—**The ability to reconstruct gastric electrical activity (termed slow waves) non-invasively from potential field measurements made on the torso surface would be a useful tool to aid in the clinical diagnosis of a number of gastric disorders. This is mathematically akin to the inverse problem of electrocardiography. To investigate this problem, an anatomically realistic torso model and an electrical stomach model were used to simulate potentials on the stomach and skin surfaces arising from normal gastric electrical activity. Gaussian noise was added to the torso potentials to represent experimental signal noise. The stomach potentials, activation profiles and gastric slow wave velocities were inversely reconstructed from the torso potentials, using the Tikhonov-Greensite inverse method with regularisation determined using an L-curve method. The inverse solutions were then compared with the known input solutions. The reconstructed solutions were able to represent the presence of multiple propagating wave fronts, determine average activation times to within 5 s and average velocities to within 1 mm/s. When more virtual body surface electrodes were used in the inverse calculations, the accuracy of the reconstructed activity improved.**

I. INTRODUCTION

THE stomach generates rhythmic electrical impulses, known as slow waves, that regulate mechanical contractions. Abnormalities in the pattern of slow wave propagation have been implicated as a disease mechanism in several functional gastric disorders such as gastroparesis and functional dyspepsia [1], [2]. The ability to non-invasively characterize slow wave activity would be beneficial for diagnosis and therapeutic strategies.

The electrogastrogram (EGG) provides a smoothed and attenuated representation of the electric potentials on the skin surface due to the slow wave activity occurring at the stomach level. However, its interpretation to date has largely been restricted to the analysis of the dominant frequency of the signals. The EGG has also gained limited clinical acceptance. However, in the cardiac field, the electrocardiogram (ECG) is widely accepted as a diagnostic tool and algorithms to reconstruct the electrical activity of heart from the body surface measurements are widely used in research. Despite the inverse problem being non-unique and ill-posed [3] algorithms have been able to successfully characterize electrical activity of the heart using body surface measurements and an accurate torso model. Recently, several studies [4]-[7] have reconstructed activation time maps and validated the results against experimental measurements. Similar approaches have yet to be applied to the gastrointestinal field.

Gastric slow wave activity has very different characteristics to cardiac activity. In humans slow waves initiate in the greater curvature in the mid-corpus region of the stomach at a frequency of approximately 3 cycles per min (cpm). The slow waves organize into a ring and propagate longitudinally down the stomach towards the pylorus. Due to the slow conduction velocity of the slow waves, up to 3 slow wave events can be present in the stomach at any point in time. In contrast, the normal heart has only one wave front present at any one time, with a frequency of approx 60 cpm. In addition, the main stomach axis is generally oriented in the anterior/posterior direction. This means that the body surface recordings may be biased towards the activity located at the antrum of the stomach.

In this study we investigated the use of a potential based inverse algorithm to reconstruct and resolve the presence of multiple simultaneous gastric slow waves using simulated data.

II. METHODS

A. Geometric Models

The anatomical model used in this study was derived from the Visible Human dataset [8], [9]. The model consisted of boundary element surfaces representing the stomach and skin. The meshes were interpolated using cubic Hermite basis functions. The stomach and skin surfaces had 626 and 290 nodes respectively.

Manuscript received March 26, 2011. This work was supported in part by the NIH (R01 DK64775) and the Health Research Council of New Zealand.

J. H. K. Kim is with the Auckland Bioengineering Institute, The University of Auckland, Auckland, New Zealand (phone: +649-373-7599 (ext. 85353); fax: +649-367-7157 ; e-mail: juliana.kim@auckland.ac.nz).

A. J. Pullan is with the Department of Engineering Science and the Auckland Bioengineering Institute, The University of Auckland, Auckland, New Zealand and Department of Surgery, Vanderbilt University, Nashville, TN (e-mail: a.pullan@auckland.ac.nz).

L. K. Cheng is with the Auckland Bioengineering Institute, The University of Auckland, Auckland, New Zealand (e-mail: l.cheng@auckland.ac.nz).

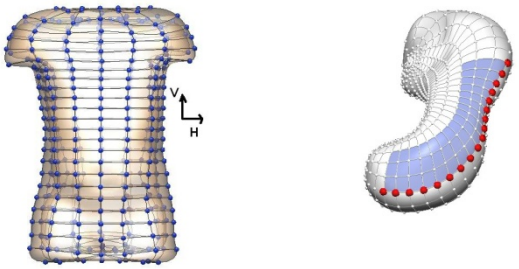

(a) (b)

Fig. 1. Boundary element models of the (a) skin and (b) stomach surfaces. In (b), the highlighted (red) nodes and shaded area (blue) in the stomach are the location of the electrodes and the area used for comparing activation times as shown in Fig. 4 and Fig. 6, respectively.

B. Gastric Electrical Sources

The underlying activity was represented by a sequence of moving dipoles. In this study up to 3 simultaneous waves were present which mimics the recent high-resolution mapping studies [10]-[12]. Each wave was derived from a detailed simulation of slow wave activity on the visible human stomach previously described [13] and was approximated by a single moving dipole. A new dipole source began in the pacemaker region when a previous dipole was approximately 37% down the length of the stomach. The relative location of the dipole sources are shown in Fig. 2.

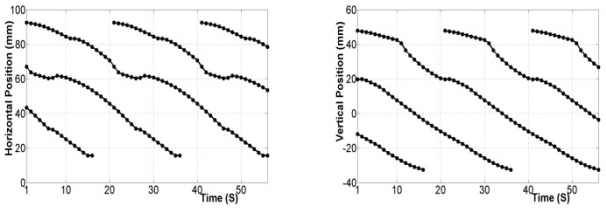

(a) (b)

Fig. 2. Location of dipole sources as a function of time in the (a) horizontal and (b) vertical directions which are represented as H and V in Fig.1(a), respectively. For the majority of the time period three simultaneous waves are present in the stomach.

C. Surface Electrodes

The gastric sources were used to simulate the potential solutions at either 84 or 204 electrodes spread uniformly over approximately 30% or 70% of the skin surface respectively. The virtual electrode locations are shown in Fig. 3.

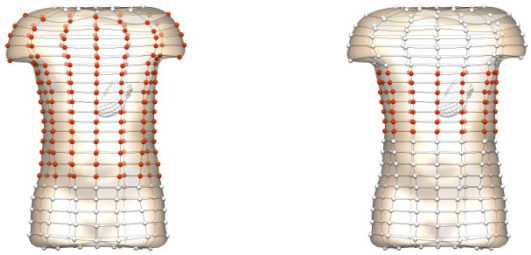

(a) 204 Elect. (b) 84 Elect.

Fig. 3. The location of the (a) 204 and (b) 84 virtual torso electrodes are shown by the highlighted (red) spheres. The simulated electrogastrograms at these electrodes were then used to reconstruct the stomach potentials.

D. Forward and Inverse Solutions

Methods mathematically similar to those used in cardiac forward/inverse simulations were used to compute potentials on the stomach and skin surfaces [14]. In our case, the epicardial surface was replaced with the surface of the stomach and the source model used consisted of the multiple dipole sources described Fig. 2.

A transfer matrix (A) that mapped the potentials on the stomach to the potentials on the skin surface was constructed using methods outlined in [14]. The inverse solution used the transfer matrix to reconstruct the stomach potentials and the method was based on solving a time series of independent quasi-static problems in the form

$$\phi_S = A^*_{\lambda_t} \phi_B \tag{1}$$

where $A^*_{\lambda_t}$ is the regularized inverse transfer matrix and ϕ_B and ϕ_S are noise corrupted body surface and stomach surface potential distributions at time t, respectively.

Gaussian noise (0.01 mV RMS approximately 10% of the average peak to peak signal) was added to the simulated body surface potentials to represent signal noise that would be present in a typical experimental setup. Using these body surface potentials, the stomach potentials were reconstructed on the stomach surface using the Tikhonov-Greensite inverse method [15], [16] with regularisation determined using an L-curve method [17].

The accuracy of the reconstructed stomach potentials was evaluated by comparing with the known stomach activation profiles, wave speeds and wave front locations. The activation time errors were calculated using the RMS (2) and relative RMS (3) metrics defined by:

$$\sqrt{\frac{\sum_{i=1}^{N}(\tau_F^i - \tau_I^i)^2}{N}} \tag{2}$$

$$\sqrt{\frac{\sum_{i=1}^{N}(\tau_F^i - \tau_I^i)^2}{\sum_{i=1}^{N}(\tau_F^i)^2}} \tag{3}$$

where τ_F^i and τ_I^i are activation times for the forward and inverse solutions at node i and N is the total number of comparison sites.

III. Results

A. Propagation patterns

The potential traces at 18 stomach locations (highlighted in red in Fig. 1(b)) from the forward solution and inverse solutions are shown in Fig 4. Stacked electrogram plots were used to track the propagation down the length of the stomach. The maximum negative slopes were calculated at each signal and the locations representing the locations of the underlying wave fronts were marked by black squares. The wave front locations were then grouped with their nearest neighbors to indicate the propagation of the wave front down the length of

the stomach. Due to errors in the inverse solutions obtained with 84 electrodes, the location of the wave front from the third to fourth electrode was chosen manually (indicated as a blue arrow shown in Fig. 4(c)). Fig. 4 shows that multiple slow wave events were able to be resolved and similar patterns were obtained when either using 204 or 84 electrodes. Results tended to be more accurate as the sources moved closer to the antrum (bottom) of the stomach.

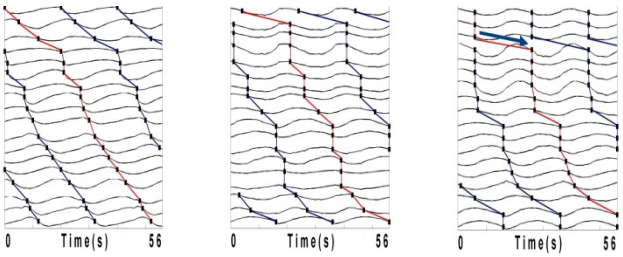

(a) Forward (b) 204 Elect. (c) 84 Elect.

Fig. 4. Stacked electrogram plot of 18 stomach surface nodes (shown in Fig. 1(b)) over a period of 56 seconds. Shown are (a) the known forward potential traces and the reconstructed traces using (b) 204 and (c) 84 virtual torso electrodes as shown in Fig. 3. The solid lines track the points of maximum negative potential representing the location of the wave front. The 3 simultaneous waves were clearly present when the signals were reconstructed using 204 electrodes, but not when 84 electrodes were used.

The RMS and relative RMS errors for activation times at 72 stomach surface nodes (in the highlighted region in Fig. 1(b)) are presented in Fig. 5(a). The average velocities of one slow wave were calculated and are presented in Fig. 5(b). The activation times reconstructed on the anterior surface were calculated to be within 5 s or 15% of the known solution. Average slow wave velocities were calculated to within 1 mm/s. However, the large standard deviations indicated that the velocities were variable down the length of the stomach.

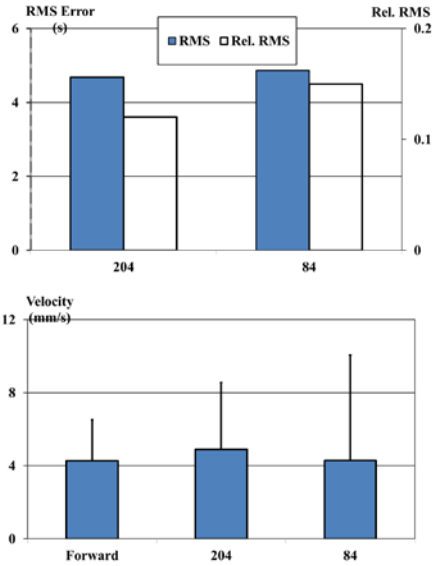

Fig. 5. Accuracy of reconstructed (a) activation times and (b) velocities compared with the forward solutions when using either 204 or 84 virtual torso electrodes. Velocities were calculated along the red electrodes shown in Fig. 1(b).

B. *Wave Front Locations*

The relative locations of the wave fronts at a particular time instance are shown in Fig. 6. The shaded regions represent areas that were activated between 22 and 28 s. The forward and inverse solution using 204 virtual torso electrodes showed the presence of 3 individual waves. However, when only 84 virtual electrodes were used, the inverse solution showed that only 2 waves could be distinguished.

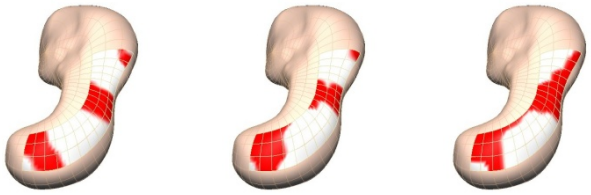

(a) Forward (b) 204 Elect. (c) 84 Elect.

Fig. 6. Relative location of wave fronts at a particular instant in time. Shown are (a) the known forward solution activation map at 25 s and the corresponding maps reconstructed using (b) 204 and (c) 84 electrodes. The shaded region (red) shows the location of the wave front.

IV. Discussion

We have presented results showing the feasibility for using cardiac based inverse algorithms to reconstruct gastric electrical activity from simulated electrograms. This study is the first known attempt to reconstruct the multiple wave fronts in the stomach from EGG signals. The results presented here demonstrate that it is possible to reconstruct similar wave front distributions to the known solutions in the presence of Gaussian signal noise.

Although mathematically the techniques used in this study are similar to those for cardiac inverses, fundamental differences remain. These include the different topology and orientation of the stomach and the presence of multiple discrete wave fronts in the stomach. The orientation of the main axis of the stomach in the anterior/posterior direction means sources near the antrum are likely to dominate the signals measured on the anterior skin surface. It may be possible that "deeper" sources are hidden by the sources located closer to the skin surface. In addition, due to the presence of multiple waves moving down the stomach axis, sufficient resolution is required at the stomach surface to resolve each of these individual waves.

The inverse solutions had average activation time and velocity errors of 5 s and 1mm/s when either 204 or 84 virtual torso electrodes were used. The accuracy of the inverse solutions improved when more torso surface electrodes were used and when the most distal wave front was located nearer to the antrum. This may be due to the fact that the stomach antrum is located close to the anterior of the torso surface, resulting in a larger signal on the torso surface.

There was difficulty in distinguishing waves in the upper stomach when using 84 virtual electrodes. This was because a section of the inversely-reconstructed stomach electrodes had similar activation times (as shown in Fig. 4(c)). If the wave front locations from the third to fourth electrodes were not manually corrected, only 2 simultaneous waves would be

detected. However, 3 simultaneous waves were clearly identified when inverse solutions were calculated using 204 virtual torso electrodes.

In this study, the velocities were calculated only in the long axis of the stomach. As such only one component of the velocity field was considered. However, in reality the propagation velocities of the slow waves should be considered in a 2 dimension.

This study used only one inverse algorithm – namely the Tikhonov-Greensite inverse method with regularisation determined using an L-curve method. Additional methods such as Tikhonov, Truncated Singular Value Decomposition (TSVD) and Greensite-TSVD and different regularization methods (zero-crossing, optimal, composite residual and smoothing operator) should be investigated to see what improvement, if any, they offer. A systematic study is also needed to quantify the effects of geometric and signal errors on the accuracy of the inverse solutions.

Finally, validating these methods experimentally by obtaining simultaneous recordings on the stomach and body surface should be conducted. However, such experiments are both technically and logistically challenging and even in the cardiac field similar studies are rarely performed.

V. Conclusion

This study demonstrates that potential based inverse methods are capable of reconstructing multiple slow wave events in the stomach from EGG signals. In the future such methods may be a useful adjunct in diagnosing electrical dysrhythmias in the gastrointestinal system.

References

[1] Z. Lin, E. Y. Eaker, I. Sarosiek, and R. W. McCallum, "Gastric myoelectrical activity and gastric emptying in patients with functional dyspepsia", *Am. J. Gastro.*, vol. *94*, no.2, pp. 2384-2389, 1999.

[2] Z. Lin, R. W. McCallum, B. D. Schirmer, and J. D. Chen, "Effects of pacing parameters on entrainment of gastric slow waves in patients with gastroparesis", *Am. J. Physiol..*, vol. *274*, pp. 186-191, 1998.

[3] J. Hadamard., "Leactures on Cauchy's Problems in Lenear Partial Differential Equations", *Yale University Press*, 1923.

[4] L. K. Cheng, G. B. Sands, R. A. French, S. J. Withy, S. P. Wong, M. E. Legget, W. M. Smith, and A. J. Pullan, "Rapid construction of a patient specific torso model from 3D ultrasound for noninvasive imaging of cardiac electrophysiology", *Med. Biol. Eng. Comput.*, vol. 43, pp. 325-330, 2005.

[5] C. Han, "Noninvasive Three-Dimensional Cardiac Activation Imaging From Body Surface Potential Maps: A Computational and Experimental Study on a Rabbit Model", *IEEE Trans. Med. Imaging*, vol. 27, pp. 1622-1630, 2008.

[6] Z. Liu, "Noninvasive Reconstruction of Three-Dimensional Ventricular Activation Sequence From the Inverse Solution of Distributed Equivalent Current Density", *IEEE Trans. Med. Imaging*, vol. 25, pp. 1307-1318, 2006.

[7] C. Ramanathan, R. N. Ghanem, P. Jia, K. Ryi, and Y. Rudy, "Noninvasive electrocardiographic imaging for cardiac electrophysiology and arrhythmia", *Nat. Med.*, vol. 10, pp. 422–428, 2004.

[8] M. L. Buist, L. K. Cheng, K. M. Sanders, and A. J. Pullan, "Multiscale modelling of human gastric electric activity: can the electrogastrogram detect functional electrical uncoupling?", *Exp. Physiol*. vol. 91, no. 2, pp. 383–390, 2006.

[9] V. Spitzer, M. J. Ackerman, A. L. Scherzinger, and D. Whitlock. „The visible human male: a technical report", *J. Am. Med. Inform. Assoc*. vol. 3, no. 2, pp. 118–130, 1996.

[10] J. U. Egbuji, G. O'Grady, P. Du, L. Cheng, W. J. Lammers, J. A. Windsor and A. J. Pullan, "Origin, propagation and regional characteristics of porcine gastric slow wave activity determined by high-resolution mapping", *Neurogastroenterol. Motil.*, vol. 22, pp. 292-300, 2010.

[11] G. O'Grady, P. Du, L. Cheng, J. U. Egbuji, W. J. Lammers, J. A. Windsor and A. J. Pullan, "The origin and propagation of human gastric slow wave activity defined by high-resolution mapping", *Am. J. Physiol. Gastrointest. Liver Physiol.*, vol. 299, pp. 582-592, 2010.

[12] Lammers, W. J., L. Ver Donck, B. Stephen, D. Smets, and J. A. Schuurkes. "Origin and propagation of the slow wave in the canine stomach: the outlines of a gastric conduction system", *Am. J. Physiol. Gastrointest. Liver Physiol.,* vol. 296, no. 6, pp. 1200–1210, 2009.

[13] J. H. K. Kim, L.A. Bradshaw, A. J. Pullan and L. K. Cheng, "Characterization of Gastric Electrical Acitivity using Magnetic Field Measurements: A Simulation Study", *Annals. of Biomed. Eng*., vol. 38, pp. 177-186, 2010.

[14] A. J. Pullan, L. K. Cheng, M. P. Nash, C. P. Bradley, and D. J. Paterson, "Noninvasive electrical imaging of the heart: Theory and model development", *Ann. Biomed. Eng.*, vol. 29, pp. 817–836, 2001.

[15] L. K. Cheng, J. M. Bodley, and A. J. Pullan, "Comparison of potential and activation based formulations for the inverse problem of electrocardiology", *IEEE Trans. Biomed. Eng.*, vol. 50, pp. 11–22, 2003.

[16] F. Greensite, "An Improved Method for Estimating Epicardial Potentials from the Body Surface", *IEEE Trans. Biomed, Eng.*, vol. 45, pp. 98-104, 1998.

[17] P. C. Hansen and D. P. O'Leary, "The use of the L-curve in the regularization of discrete ill-posed problems", *SIAM Journal on Scientific Computing*, vol. 14, pp. 1487-1503, 1993.